Ab initio vibrational and dielectric properties of the chalcopyrite $CuInSe_2$

Cihan Parlak and Resul Eryiğit
Department of Physics, Abant Izzet Baysal University, Bolu-Turkey, 14280
(Received 25 April 2002; published 2 October 2002)

We have performed a first-principles study of structural, dynamical, and dielectric properties of the chalcopyrite semiconductor $CuInSe_2$. The calculations have been carried out within the local density functional approximation using norm-conserving pseudopotentials and a plane-wave basis. Born effective charge tensors, dielectric permitivity tensors, the phonon frequencies at the Brillouin zone center, and mode oscillator strengths are calculated using density functional perturbation theory. The calculated properties agree with some of the infrared, Raman, and neutron measurements.

DOI: 10.1103/PhysRevB.66.165201 PACS number(s): 78.30.Hv, 63.20.Dj, 77.22.Ch

I. INTRODUCTION

The ternary I-III-VI_2 chalcopyrites form a large group of semiconductors with diverse structural, electrical, and optical properties.[1,2] One of these classes of materials, $CuInSe_2$, is considered as one of the most promising materials for the solar applications, partly because of its strong absorption under sunlight.[2]

Over the last three decades the lattice dynamical properties of $CuInSe_2$ have been investigated experimentally as well as theoretically by a number of groups. Its Brillouin zone Center (BZC) phonon frequencies have been measured by using Raman,[3,4] infrared,[3,5–9] and neutron spectroscopy.[10] Earlier theoretical studies used phenomenological lattice dynamical models, such as the Born–von Karman,[11] rigid ion,[12] Urey-Bradley force field,[13] valence force field,[11] universal force field[14] and Keating models.[15,16] Model calculations have two main drawbacks; the type of interaction they take into account might not be enough, and their interaction parameters have to be derived from a fit to experimentally measured phonon frequencies. Unfortunately, there are severe differences in the frequencies of some of the BZC modes of $CuInSe_2$, which is, generally, attributed to off-stochiometry, poor surface preparation of samples, or polarization related experimental errors. Recently, Lazewski and Parlinski[17] reported first principles calculation results of BZC phonon frequencies of $CuInSe_2$. They used a direct method where the phonon frequencies are calculated from Hellmann-Feynman forces generated by the small atomic displacements.

The first-principles investigation of phonon frequencies can be performed within a density functional perturbation theory (DFPT),[18] frozen-phonon,[19] or direct method approach. In contrast to frozen-phonon technique, the DFPT formalism has the advantage that phonons at any wave vector in the Brillouin zone are accessible. For polar crystals, there is another disadvantage of the direct method: The nonanalytic behavior of dynamical matrices as functions of the wave vector in the long-wave limit, which causes the LO-TO splitting of zone center optical modes, has to be supplied by a separate calculation using Berry's phase approach, borrowed from a density functional perturbation theory calculation, fitted to experiment, or obtained from use of an elongated supercell.[18] In contrast to the direct method of calculating the phonon frequencies, the linear response approach lets one obtain the effective charges and dielectric tensors directly. To the best of our knowledge, in all *ab initio* calculations of chalcopyrite phonon frequencies,[17,20–23] the nonanalytic term is introduced from the experimental effective charges.

In this paper, we investigate the equilibrium lattice structure, Born effective charge tensors, dielectric permitivity tensors, zone center phonon frequencies, and mode oscillator strengths of $CuInSe_2$ using the density functional and density functional perturbation theory.[18,24,25] Our aim is to help resolve the discrepancies in reported phonon frequencies and provide first principles Born effective charges and dielectric tensors.

II. METHOD OF CALCULATION

The present results have been obtained using the ABINIT code,[26] that is based on pseudopotentials and planewaves. It relies on an efficient fast Fourier transform algorithm[27] for the conversion of wave functions between real and reciprocal space, on the adaptation to a fixed potential of the band-by-band conjugate gradient method,[28] and on a potential-based conjugate-gradient algorithm for the determination of the self-consistent potential.[29]

The pseudopotentials have been generated with FHI98PP code.[30] Special care has been used in constructing the pseudopotentials, in order to avoid the occurrence of ghost states[31] and to assure an optimal transferability over a wide energy range. We find that the inclusion of semicore states, such as $3d$ Cu, greatly improves the transferability of the pseudopotentials, and is at the same time necessary to take into account the hybridization of cation semicore states with anionic p states. The inclusion of Cu d states increases the kinetic energy cutoff of the plane waves included in the calculation because of the compact nature of these orbitals. The kinetic energy cutoff needed to obtain a convergence better than 0.01 eV of both total energies is found to be equal to 45 H. The Brillouin zone is sampled by 12 special k points, which is found to be enough for convergence of static as well as response calculations.

Technical details on the computation of responses to atomic displacements and homogeneous electric fields can be found in Ref. 24, while Ref. 25 presented the subsequent

TABLE I. The coordinates of the eight atoms in the chalcopyrite $CuInSe_2$ primitive unit cell in terms of lattice vectors. The lattice vectors of the unit cell are $a_1=a(1,0,0)$, $a_2=a(0,1,0)$ and $a_3=a(0.5,0.5,0.5\eta)$ and $x=u/2$.

Atom	Coordinates
Cu_1	$(0,0,0)$
Cu_2	$(-0.25,0.25,0.5)$
In_1	$(0.5,0.5,0.0)$
In_2	$(0.25,-0.25,0.5)$
Se_1	$(x,0.125,0.25)$
Se_2	$(-(0.25+x),-0.375,0.25)$
Se_3	$(-0.125,(0.25+x),-0.25)$
Se_4	$(0.375,-x,-0.25)$

computation of dynamical matrices, Born effective charges, dielectric permittivity tensors, and interatomic force constants.

III. RESULTS

A. Atomic structure

The chalcopyrite structure (space group D_{2d}^{12}, No. 122) can be considered to be derived from the cubic zinc-blende structure (space group T_d^2) by populating one of the face-centered-cubic sublattice with group-VI atoms, and another one with equal amounts of group-I and -III atoms in a regular fashion. In general, I-VI and III-VI bond lengths, denoted by $d_{\text{I-}VI}$ and $d_{\text{III-}VI}$, respectively, are not equal. One consequence of having two different anion-cation bond lengths is a tetragonal distortion characterized by $u=0.25+(d_{\text{I-}VI}^2-d_{\text{III-}VI}^2)/a^2$ which describes the repositioning of the anions in the x-y plane, where a is the lattice constant in the x or y direction. The second consequence of differing anion-cation bond lengths is a deformation of the unit cell to a length c which is generally different from $2a$. This tetragonal distortion is characterized by the quantity $\eta=c/a$.

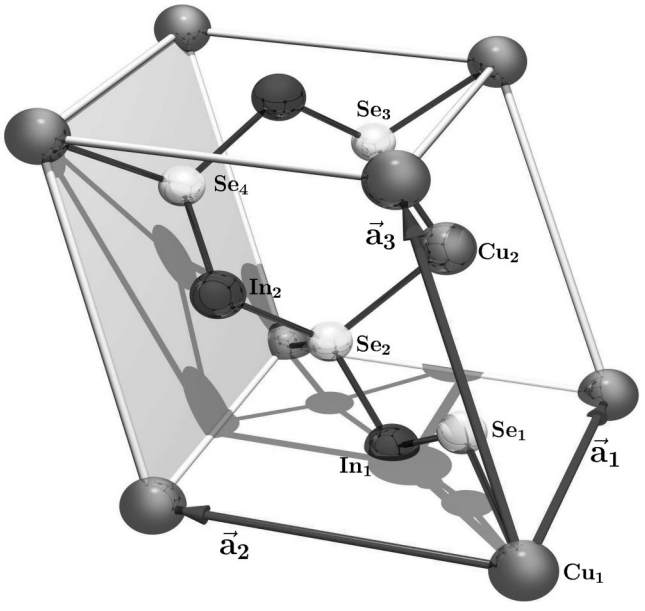

FIG. 1. Primitive unit cell of chalcopyrite $CuInSe_2$.

TABLE II. Calculated structural parameters of $CuInSe_2$ compared to experimental and other theoretical calculations. a is the lattice constant in the x or y direction, $\eta=c/a$ and u is the tetrahedral distortion parameter. a is in atomic units while η and u are unitless.

	Theory		Experiment	
	This work	Ref. 17	Ref. 32	Ref. 33
a	10.51	11.02	10.91	10.93
η	2.002	1.994	2.010	2.008
u	0.237	0.222	0.235	0.224

The unit vectors of the primitive cell are $(a,0,0)$, $(0,a,0)$, and $(a/2,a/2,\eta a/2)$ and the coordinates of the atoms in reduced coordinates forming the unit cell are displayed in Table I (also see Fig. 1). The lattice parameters are determined from atomic and structural relaxation, and compared to available experimental values and theoretical calculation of Ref. 17 in Table II. Considering the fact that the zero-point motion and thermal effects are not taken into account, the calculated a, η and u values agree with the experimental values quite well.

B. Born effective charge tensors

For insulators, the Born effective charge tensor for atom κ, $Z^{\star}_{\kappa,\beta\alpha}$, quantifies, to linear order, the polarization per unit cell, created along the direction β when the atoms of sublattice κ are displaced along the direction α, under the condition of zero electric field. It can be calculated from the Berry phase or from perturbation theory.

Our results for the dynamical effective charges of $CuInSe_2$ are presented in Table III. Because of finite k-point

TABLE III. Calculated Born effective charges of $CuInSe_2$. The eigenvalues of the symmetric part of $Z^{\star}$ are given in brackets.

$Z^{\star}_{Cu_1}$	$\begin{pmatrix} 0.76 & -0.10 & 0.00 \\ 0.10 & 0.76 & 0.00 \\ 0.00 & 0.00 & 0.74 \end{pmatrix}$	$\begin{bmatrix} 0.76 \\ 0.76 \\ 0.74 \end{bmatrix}$
$Z^{\star}_{In_1}$	$\begin{pmatrix} 2.52 & -0.04 & 0.00 \\ 0.04 & 2.52 & 0.00 \\ 0.00 & 0.00 & 2.67 \end{pmatrix}$	$\begin{bmatrix} 2.52 \\ 2.52 \\ 2.67 \end{bmatrix}$
$Z^{\star}_{Se_1}$	$\begin{pmatrix} -1.53 & 0.00 & 0.00 \\ 0.00 & -1.75 & 0.62 \\ 0.00 & 0.66 & -1.71 \end{pmatrix}$	$\begin{bmatrix} -2.37 \\ -1.53 \\ -1.09 \end{bmatrix}$
$Z^{\star}_{Se_3}$	$\begin{pmatrix} -1.75 & 0.00 & 0.64 \\ 0.00 & -1.53 & 0.00 \\ 0.67 & 0.00 & -1.71 \end{pmatrix}$	$\begin{bmatrix} -2.37 \\ -1.53 \\ -1.09 \end{bmatrix}$

sampling there is a deviation from charge neutrality which is less than 0.01 electron for the unit cell. The form of effective charge tensor is determined by the site symmetry of the ions. $Z^\star$ of cations, which have same site symmetry (they are located at $4a$ and $4b$ Wyckoff positions) are almost diagonal with an anisotropy of 0.03 for Cu and 0.06 for In. Selenium ions are located at lower symmetry sites ($8d$ positions), and as a result their effective charge tensors have nonequivalent diagonal components as well as sizable off-diagonal components. The tetrahedral shifting of anion atoms creates four different configurations for these atoms and the resulting effective charge tensor elements can be divided into two classes according to the direction of the tetrahedral shifting being along the x or y direction. $Z^\star_{\mathrm{Se},zz}=-1.71$ for all anions, while $Z^\star_{\mathrm{Se},xx}$ and $Z^\star_{\mathrm{Se},yy}$ take the value -1.53 or -1.75 depending on the direction of u. Also, depending on the u distortion being along the x or y direction, the off-diagonal components $Z^\star_{\mathrm{Se},zx}$, $Z^\star_{\mathrm{Se},xz}$ or $Z^\star_{\mathrm{Se},yz}$, and $Z^\star_{\mathrm{Se},zy}$ are different from zero.

Tanino *et al.*[4] used measured LO-TO splittings and a model to estimate the Born effective charges of $CuInSe_2$, which were assumed to be isotropic. One further assumption of their calculation was the effective charge of selenium, extrapolated from the effective charges of ZnSe and CdSe as -0.865 [It should be mentioned that the dynamical effective charges of zinc-blende semiconductors are in the range 1.8–2.7 (Ref. 34).] Based on this value, they obtained $Z^\star_{\mathrm{Cu}}=0.475$ and $Z^\star_{\mathrm{In}}=1.255$. A qualitative comparison of these experimental values and average of the diagonal components of our calculated effective charge tensors can be made. From Table III, the average for Se is -1.66. If one takes this value in Tanino *et al.*'s model than the effective charges for Cu and In become 0.86 and 2.46, respectively. These values would agree fairly well with our calculations. But, one should keep in mind that, although this comparison involves numbers, it is only qualitative in nature.

The Born effective charge tensors of cations show very little anisotropy. If one assumes a Cu(+1)-In(+3)-Se(-2) static ionic configuration for $CuInSe_2$ compound, then the calculated Born effective charges are not very different than the static charges. The anomalous Born effective charge phenomena, which is common for perovskites,[35] is not seen for chalcopyrites.

C. Phonons

Since the body-centered tetragonal unit cell of the chalcopyrite structure has eight atoms, there are a total of 24 modes of vibration. A detailed discussion of group theoretical properties of $CuInSe_2$ zone center phonons can be found in Ref. 4. The irreducible representation at the center of the Brillouin zone is

$$\Gamma_{\mathrm{opt}}=1\Gamma_1\oplus 2\Gamma_2\oplus 3\Gamma_3\oplus 3\Gamma_4\oplus 6\Gamma_5$$

for optical modes, and

$$\Gamma_{\mathrm{aco}}=1\Gamma_4\oplus 1\Gamma_5$$

for acoustic modes. Optical modes having Γ_1 and Γ_2 symmetry involve only displacement of anions. Γ_3, Γ_4 and Γ_5 modes include displacement of cations, as well. Both Γ_4 and Γ_5 modes belong to vector transforming representation, and are thus IR active. Inclusion of the long range polarization interaction results in splitting of the Γ_4 and Γ_5 modes into TO and LO components giving nine polar vibrations [three with polarization along c (Γ_4 modes) and six along x or y (Γ_5)]. This results in different numbers of IR modes being active for $E\|c$ and $E\perp c$. Except for modes of Γ_2 symmetry, all optical modes are Raman active.

In Table IV our calculated zone center phonon frequencies and their symmetry assignments are displayed and compared with the results of first principles calculation of Ref. 22 and infrared,[3,5–9] Raman,[3,4] and neutron scattering[10] measurements. For some of the modes there are large differences between the reported experimental frequencies, for example, one of the Γ_4^{LO} mode frequencies ranges from 6.85 (Ref. 9) (IR measurement) to 8.21 (Ref. 3) THz (IR measurement). The reason for some of the discrepancies might be the imperfect polarization conditions with optical experiments which may result in incorrect mode assignments and in shifts of mode frequencies if modes with similar oscillator strengths and frequencies are present in the two polarization directions. Also, problems in surface preparation is cited as one of the important source of differences. In Table IV we also display the absolute value rms relative deviation of our results and results of Ref. 22. The rms relative deviation of both results with Ref. 9 is around 30%, which is very high. This suggests that, at least some of the frequencies (especially mid range Γ_5 and Γ_4 modes) reported in Ref. 9 are not phonon modes of a perfect $CuInSe_2$ crystal. Also, Raman measurements of Ref. 3 seem to be too high for the highest frequency Γ_5 mode. Based on a comparison of rms relative deviations, our results are somewhat better than those reported in Ref. 17, especially for low temperature Raman measurements of Tanino *et al.*[4]

D. Lattice dielectric tensors

The form of the dielectric tensor is determined by the symmetry of the crystal. Our calculated electronic (ϵ_∞) and static (ϵ_0) dielectric tensors have two independent components $\epsilon^{\|}$ and $\epsilon^{\perp}$ along and perpendicular to the c axis, respectively. While the electronic dielectric tensor is almost isotropic, ϵ_0 has a small ($\approx 3.4\%$) anisotropy, which is consistent with the fact that for $CuInSe_2$ tetragonal distortion is very small ($\eta=c/a\approx 2$).

We display our calculated dielectric tensor components along with model calculations of Ref. 36, and experimentally available values in Table V. The averages of ϵ_∞ and ϵ_0, obtained from the expression ϵ_∞ (or ϵ_0) $=(2\epsilon_\infty^{\perp}+\epsilon_\infty^{\|})/3$, are also shown in this table. Available experimental data for high frequency and static dielectric constants of $CuInSe_2$ show considerable differences. The sources of these discrepancies are similar to the reasons mentioned in the discussion of phonon frequencies. Reported values for ϵ_∞ ranges from 6.35 (Ref. 37) to 11.8 ± 2.[38] One important factor in determining the dielectric constant is the model dielectric function used to

TABLE IV. Zone center phonon frequencies of $CuInSe_2$ (in THz).

Mode	Theoretical results		Experimental results						
	This work	Ref. 17	IR (Ref. 3)	IR (Refs. 5–8)	IR (Ref. 9)	R (Ref. 3)	R^a	R^b	N (Ref. 10)
Γ_1	5.54	5.31				5.58	5.28	5.34	5.34
Γ_2	5.99	5.59							5.90
	5.03	5.26							4.83
	6.84	6.60				6.87			6.20
Γ_3	5.52	4.87				4.74		5.37	4.76
	2.10	2.31				3.51		2.01	1.85
Γ_4LO									
TO	7.25	7.13	8.21	6.96	6.85		6.99	6.99	7.15
	6.84	6.48	7.44	6.42	6.25		6.45	6.51	
	6.11	6.45	5.88	5.79	5.07	5.82	5.94	6.00	5.82
	5.93	5.93	5.64	5.43	4.89	5.82	5.94	5.31	
	2.12	2.18		1.95	2.36	2.88	2.13	2.16	1.65
	2.10	1.99		1.92	2.11	2.88	2.10	2.10	
Γ_5 LO	7.11	7.32	8.21	6.87	6.82	8.24	6.90	6.99	6.44
TO	6.68	6.45	7.44	6.39	6.12	7.55	6.51	6.51	
	6.70	6.43			5.22			6.90	5.95
	6.57	6.28			4.86			–	
	6.21	6.11	5.73	6.36	3.85	5.73	6.33	6.48	5.42
	6.13	5.91	5.64	6.21	3.66	5.73	6.33	6.33	
	4.65	4.49	4.59	5.49	3.48			5.64	4.07
	4.65	4.49	4.59	5.37	3.24			5.64	
	2.27	2.14	2.34		2.32	2.34		2.34	2.09
	2.24	2.11	2.34		2.32	2.34		2.13	
	1.77	1.57		2.01	1.71	1.83	1.80	1.80	1.59
	1.77	1.56		1.92	1.66	1.83	1.74	1.83	
				rms relative deviations					
This work		0.058	0.077	0.084	0.285	0.150	0.030	0.070	0.112
Ref.17	0.058		0.091	0.116	0.264	0.155	0.060	0.099	0.094

[a]Reference 4 (at 100 K).
[b]Reference 4 (at 300 K).

fit the infrared reflectivity data and fitting process itself. We have found that the product form of model dielectric function could fit the IR data of Ref. 9 much better than their report. This fit gives ϵ_∞ around 9.0. Since it is well known that density-functional-theory–local-density-approximation (DFT-LDA) calculations overestimate the value of high frequency dielectric constant, our calculations agree well with Wasim's data[39] ($\epsilon_\infty = 8.1 \pm 1.4$). Similarly, experimental ϵ_0 values range from 7.67 (Ref. 37) to 16.0.[8] Again, taking into account the overestimation of DFT-LDA approach, the expected theoretical ϵ_0 would be around 10.0.

TABLE V. Static and high frequency dielectric tensor components of $CuInSe_2$.

	$\epsilon_\infty^\parallel$	$\epsilon_\infty^\perp$	ϵ_∞	$\epsilon_0^\parallel$	$\epsilon_0^\perp$	ϵ_0
This work	8.48	8.64	8.59	10.71	10.34	10.46
Ref. 36	7.5	7.6	7.57	10.8	11.0	10.93
Ref. 5	8.5	9.5	9.18	15.2	16.0	15.73
Ref. 9	6.00	6.86	6.57	12.09	16.63	15.12
Ref. 37	3.64	7.7	6.35	4.31	9.36	7.67
Ref. 7	7.88	7.66	7.73			
Ref. 38			11.8 ± 2.0			
Ref. 39			8.1 ± 1.4			13.6 ± 2.4
Ref. 40			9.18			

The static dielectric tensor can be decomposed in the contributions of different modes as[24]

$$\epsilon^0_{\alpha\beta} = \epsilon^\infty_{\alpha\beta} + \frac{4\pi}{\Omega_0} \sum_m \frac{S_{m,\alpha\beta}}{\omega_m^2}, \tag{1}$$

where Ω_0 is the volume of the primitive unit cell, ω_m is the frequency of mode m and $S_{m,\alpha\beta}$ is the oscillator strength tensor which is related to eigendisplacements $U_m(\kappa\alpha)$ and Born effective charge tensors by

$$S_{m,\alpha\beta}=\left(\sum_{\kappa\alpha'} Z^{\star}_{\kappa,\alpha\alpha'}U^{\star}_{m}(\kappa\alpha')\right)\left(\sum_{\kappa'\beta'} Z^{\star}_{\kappa',\beta\beta'}U^{\star}_{m}(\kappa'\beta')\right). \tag{2}$$

Similarly, one can define a mode-effective charge tensor as

$$Z^{\star}_{m,\alpha}=\frac{\sum_{\kappa\beta} Z^{\star}_{\kappa,\alpha\beta}U_{m}(\kappa\beta)}{\left[\sum_{\kappa\beta} U^{\star}_{m}(\kappa\beta)U_{m}(\kappa\beta)\right]^{1/2}}. \tag{3}$$

For IR active modes the relevant components of the oscillator strength tensor and the magnitude of the mode effective charge tensor along with experimental oscillator strength data from Refs. 6 and 9 are displayed in Table VI. For both Γ_4 and Γ_5 symmetry higher frequency modes have higher mode effective charges and oscillator strengths. Our calculated oscillator strength values of Γ_4 modes show a reasonable agreement with both sets of experiments. However, for Γ_5 modes not even a qualitative agreement can be found with Ref. 6. Since Syrbu *et al.* were able to detect only three modes of Γ_5 symmetry, their S_m values are result of a fit with only three oscillator strength parameters. Except for the highest frequency mode, agreement is fair.

TABLE VI. Oscillator strength tensor S_m (in 10^{-4} m^3/s^2), magnitude of mode-effective charge vectors $Z^{\star}_m$ and LO frequencies ω_m (in THz) of $CuInSe_2$.

	S_m			$Z^{\star}_m$	ω_m
	Theory	Ref. 6	Ref. 9		
Γ_4	1.80	0.24	2.03	1.14	2.10
Γ_4	9.56	8.50	9.24	3.03	6.12
Γ_4	9.62	6.94	10.02	4.26	6.84
Γ_5	0.21		0.57	0.22	1.78
Γ_5	0.00		2.12	0.32	2.26
Γ_5	0.39		2.32	0.20	4.65
Γ_5	6.44	2.99	2.45	2.02	6.13
Γ_5	9.62	6.67	6.47	3.52	6.57
Γ_5	8.27	2.42	15.09	3.05	6.68

IV. CONCLUSION

We have investigated dynamical properties, such as the Born effective charge tensor, the Brillouin zone center phonon frequencies, and static and the high frequency dielectric tensors of the ternary semiconductor $CuInSe_2$, within the density functional perturbation theory. From a comparison of previous results and our first principles results with several sets of experimental data, one can claim that some of the reported zone center mode frequencies do not belong to chalcopyrite $CuInSe_2$. Also, our calculated static and high frequency dielectric tensors help to resolve the discrepancies in the reported experimental data. We have also computed mode oscillator strengths and mode effective charges of the infrared active modes, and found fair agreement with some of the experiments.

ACKNOWLEDGMENT

We thank the Bilkent University High Performance Computing Center for allocation of computing time on their machines.

[1] A. M. Gaber, J. R. Tuttle, D. S. Albin, A. L. Tennant, and M. A. Contreras, in *12th NREL Photovoltaic Program Review*, edited by R. Noufi, AIP Conf. Proc. No. 306 (AIP, New York, 1994), p. 59.
[2] R. W. Birkmire and E. Eser, Annu. Rev. Mater. Sci. **27**, 625 (1997).
[3] J. N. Gan, J. Tauc, V. G. Lambrecht, and M. Robbins, Phys. Rev. B **13**, 3610 (1976).
[4] H. Tanino, T. Maeda, H. Fujikake, H. Nakanishi, S. Endo, and T. Irie, Phys. Rev. B **45**, 13323 (1992).
[5] V. Riede, H. Sobotta, H. Neumann, H. X. Nguyen, W. Möller, and G. Kühn, Solid State Commun. **28**, 449 (1978).
[6] H. Neumann, H. Sobotta, V. Riede, B. Schumann, and G. Kühn, Cryst. Res. Technol. **18**, K90 (1983).
[7] H. Neumann, R. D. Tomlinson, W. Kissinger, and N. Avgerinos, Phys. Status Solidi B **118**, K51 (1983).
[8] H. Neumann, Sol. Cells **16**, 399 (1986).
[9] N. N. Syrbu, M. Bogdanash, V. E. Tezlevan, and I. Mushcutariu, Physica B **229**, 199 (1997).
[10] P. Derollez, R. Fouret, A. Laamyem, B. Hennion, and J. Gonzalez, J. Phys.: Condens. Matter **11**, 9673 (1999).
[11] R. Fouret, P. Derollez, A. Laamyem, B. Hennion, and J. Gonzalez, J. Phys. (Paris) **9**, 6579 (1997).
[12] F. W. Ohrendorf and H. Haeuseler, Cryst. Res. Technol. **34**, 339 (1999).
[13] H. A. Lauwers and M. A. Herman, J. Phys. Chem. Solids **38**, 983 (1977).
[14] J. Lazewski and K. Parlinski, Phys. Status Solidi B **218**, 411 (2000).
[15] M. Bettini, Phys. Status Solidi B **69**, 201 (1975).
[16] L. Artus, J. Pujol, J. Pascual, and J. Camassel, Phys. Rev. B **41**, 5727 (1990).
[17] J. Lazewski, K. Parlinski, B. Hennion, and R. Fouret, J. Phys.: Condens. Matter **11**, 9665 (1999).
[18] S. Baroni, S. de Gironcoli, A. dal Corso, and P. Giannozzi, Rev. Mod. Phys. **73**, 515 (2001).
[19] K. Kunc and R.-M. Martin, *Ab Initio Calculation of Phonon Spectra* (Plenum, New York, 1983), p. 65.
[20] B. B. Karki, S. J. Clark, M. C. Warren, H. C. Hsueh, G. J. Ackland, and J. Crain, J. Phys.: Condens. Matter **9**, 375 (1997).
[21] G. J. Ackland, M. C. Warren, and J. S. Clark, J. Phys.: Condens. Matter **9**, 7861 (1997).
[22] J. Lazewski and K. Parlinski, J. Phys.: Condens. Matter **11**, 9673 (1999).
[23] J. Lazewski and K. Parlinski, J. Chem. Phys. **114**, 6734 (2001).
[24] X. Gonze, Phys. Rev. B **55**, 10337 (1997).

[25] X. Gonze and C. Lee, Phys. Rev. B **55**, 10355 (1997).
[26] The ABINIT code is a common project of the Universite Catholique de Louvain, Corning Incorporated, and other contributors, URLhttp://www.abinit.org
[27] S. Goedecker, SIAM (Soc. Ind. Appl. Math.) J. Sci. Stat. Comput. **18**, 1605 (1997).
[28] M. C. Payne, M. P. Teter, D. C. Allan, T. A. Arias, and J. D. Joannopoulos, Rev. Mod. Phys. **64**, 1045 (1992).
[29] X. Gonze, Phys. Rev. B **54**, 4383 (1996).
[30] M. Fuchs and M. Scheffler, Comput. Phys. Commun. **119**, 67 (1999).
[31] X. Gonze, R. Stumpf, and M. Scheffler, Phys. Rev. B **44**, 8503 (1991).
[32] J. Parkes, R. D. Tomlinson, and M. J. Hampshire, J. Appl. Crystallogr. **6**, 414 (1973).
[33] H. W. Spiess, U. Haeberln, G. Brandt, A. Räuber, and J. Schneider, Phys. Status Solidi B **62**, 183 (1974).
[34] *Handbook of Optics*, edited by W. L. van Stryland, D. R. Williams, W. L. Wolfe, and M. Bass (McGraw-Hill, New York, 1995), Chap. 33.
[35] P. Ghosez, J.-P. Michenaud, and X. Gonze, Phys. Rev. B **58**, 6224 (1998).
[36] R. Marquez and C. Rincon, Phys. Status Solidi B **191**, 115 (1995).
[37] I. V. Bodnar, G. F. Smirnova, T. V. Smirnova, Y. A. Aleschenko, and L. K. Vodopyanov, Phys. Status Solidi B **145**, 117 (1988).
[38] C. Rincon, M. A. Arsene, S. M. Wasim, F. Voillot, J. P. Peyrade, P. Bocaranda, and A. Albacete, Matt. Letters **29**, 87 (1996).
[39] S. Wasim, Sol. Cells **16**, 289 (1986).
[40] M. F. Kotkata, K. M. Kandil, and M. S. Al-Kotb, J. Non-Cryst. Solids **205-207**, 180 (1996).